Available online at www.sciencedirect.com
SCIENCE DIRECT®
Journal of Computational Physics 194 (2004) 140–155
JOURNAL OF COMPUTATIONAL PHYSICS
www.elsevier.com/locate/jcp

A sequence of absorbing boundary conditions for Maxwell's equations

William F. Hall *, Adour V. Kabakian

HyPerComp, Inc., 31255 Cedar Valley Dr., Suite 327, Westlake Villiage, CA 91362, USA

Received 17 September 2002; received in revised form 29 July 2003; accepted 4 September 2003

Abstract

Following the scheme developed by Engquist and Majda [Math Comp. 31 (1977) 629] for first-order systems, we derive a theoretical perfectly absorbing nonlocal boundary condition for Maxwell's equations at a flat outer boundary. This condition can be approximated to any desired order by a differential equation on the boundary, and a sequence of such equations is developed here in terms of tangential derivatives of the electromagnetic fields at the boundary. The resulting set of equations, comprising Maxwell's equations in the interior together with any of the local boundary conditions, is shown to admit no exponentially growing solutions, and questions of their well-posedness are addressed.

Keywords: Absorbing boundary conditions; Maxwell's equations

1. Introduction

In their 1977 paper [1] entitled ''Absorbing Boundary Conditions for the Numerical Simulation of Waves'', Engquist and Majda construct procedures for minimizing the magnitude of waves reflected from the boundaries of a finite computational domain. The local boundary conditions that they derive are differential equations on the boundary that provide for the stability of discretized forms of the time-dependent wave equation inside the domain in the sense that they admit no exponentially growing solutions. Their analysis includes both the scalar second-order wave equation and first-order systems that are strictly hyperbolic (i.e., having no zero eigenvalues).

Maxwell's equations written as a first-order system are not strictly hyperbolic. However, plane-wave solutions for the fields can be decomposed into two sets of components that individually satisfy the scalar wave equation. In the present paper a method is presented for extending the first-order system approach to include the time-dependent form of Maxwell's equations, and vector absorbing boundary conditions of arbitrarily high order are constructed. Resolution of these conditions into their scalar wave components is

* Corresponding author. Tel.: +1-805-492-4010; fax: +1-818-865-3711.
E-mail address: wfhall@adelphia.net (W.F. Hall).

0021-9991/$ - see front matter
doi:10.1016/j.jcp.2003.09.001

found to recover the appropriate results, and the well-posedness of the mixed initial boundary value problems closed by these conditions is examined.

The need for absorbing boundary conditions of higher order has emerged from the recent development of numerical methods that employ high-order representations of the field variables inside each computational cell of a space-filling grid [3,4]. In contrast to methods that allow for no variation within a cell, these methods have been shown to preserve both the amplitude and phase of propagating waves to high accuracy over many wavelengths. In particular, low-order methods damp the waves as they propagate to and from the outer boundaries of a computational domain, thereby minimizing the effects of the numerically reflected return. High-order methods suffer nearly the full effect of these reflections.

Mur [5] applied the scalar wave results of Engquist and Majda in the special context of staggered-grid Cartesian simulation of Maxwell's equations (an integration method known as the Yee scheme [6]). Taflove [7] and others successfully exploited these boundary conditions for a variety of finite-difference time domain (FDTD) simulations. However, currently these boundary conditions have been supplanted in FDTD simulations by surrounding the domain of interest with an absorbing layer that has special properties, following the work of Berenger [8].

Berenger has taken a different approach to minimizing reflections from the computational boundary. He regards Maxwell's equations as a degenerate form of a more general set of equations having additional degrees of freedom that are only active outside the original computational domain. By choosing the parameters of the external medium appropriately, direct reflection from the interface between this medium and the interior Maxwell domain is eliminated. Further, exponential damping of the waves in this medium is achieved. A finite, but exponentially small, reflection from the outer computational boundary of this "perfectly matched" layer, or PML, is all that remains. While this approach has proven quite effective for FDTD, Abarbanel and Gottlieb [9] have shown that the resulting discretized system suffers from both exponential and long-term instabilities.

Various approaches to remove the effects of the instabilities numerically, or to replace the original PML with a different kind of strongly absorbing layer, are being actively investigated. In the meanwhile, one can use the extended Engquist–Majda boundary conditions developed here as a viable alternative. They produce reflections that are algebraically small, going as $[(1-\cos(\theta))/(1+\cos(\theta))]^{m+1}$ for the mth-order condition, where θ is the angle of incidence on the boundary.

2. Formulation

Maxwell's equations relating the time development of the electric field $\mathbf{E}$ and the magnetic field $\mathbf{H}$ in vacuum can be written in an appropriately scaled form as

$$\partial\mathbf{H}/\partial t = -\nabla \times \mathbf{E}, \tag{2.1a}$$

$$\nabla \cdot \mathbf{H} = 0, \tag{2.1b}$$

$$\partial\mathbf{E}/\partial t = \nabla \times \mathbf{H}, \tag{2.2a}$$

$$\nabla \cdot \mathbf{E} = 0. \tag{2.2b}$$

To make contact with standard SI units, one can consider time to be measured in distance units of ct, where c is the speed of light, and $\mathbf{E}$ to be measured in volts per meter divided by Z_0, the impedance of free space. The divergence conditions (2.1b), (2.2b) can be regarded as initial conditions on the fields, since the time derivative of either divergence vanishes by reason of Eqs. (2.1a), (2.2a).

Adopting the notation conventions of Engquist and Majda [1], the Maxwell system (2.1a), (2.2a) is recast in the form

$$\partial u/\partial t = (A_1\,\partial/\partial x + A_2\,\partial/\partial y + A_3\,\partial/\partial z)u, \tag{2.3}$$

where $u = (\mathbf{H}, \mathbf{E})^{\mathrm{T}}$ is a column vector of six unknowns, and each A_i is a 6×6 singular matrix with constant elements. (In what follows, we shall continue to use bold print to denote physical vectors.)

The plane wave solutions to these equations have $\mathbf{E} \cdot \mathbf{H} = 0$, and both vectors are orthogonal to the direction of propagation of the wave. Along a given direction, there are two eigenvalues of the system corresponding to positively propagating waves (with unit wavespeed), two eigenvalues corresponding to waves propagating in the opposite direction, and two zero eigenvalues. It is these zero eigenvalues that prevent the direct application of the method developed by Engquist and Majda for first-order systems to Maxwell's equations.

A formal solution for this difficulty is to modify the equations appropriately so that all eigenvalues are real and nonzero. That is the approach adopted here. The resulting system can then be transformed to isolate a subspace corresponding to waves incoming along a given direction. Requiring that the components of u corresponding to this subspace vanish at the boundary leads to a nonlocal boundary condition that is theoretically perfectly absorbing for the modified system [1]. However, for this procedure to yield a valid result for the unmodified system, the transformation must at least remain well defined in the limit that the modification is removed.

Finally, one can approximate the nonlocal condition using local derivatives of u at the boundary. As Engquist and Majda demonstrate, not every consistent approximation leads to a well-posed system of differential equations for the finite domain. In the last three sections of this paper an infinite sequence of such approximations is constructed that satisfies this criterion, and the behavior of a discrete implementation is explored for a spherical test case using the Runge–Kutta discontinuous Galerkin approach [3] to provide the high-order representation.

3. The modified equations

As a convenience for later developments, we shall replace $\mathbf{E}$ and $\mathbf{H}$ as the unknowns in Eq. (2.3) by the characteristic combinations corresponding to waves propagating parallel to the unit normal $\boldsymbol{\xi}$ at the outer boundary of the computational domain:

$$\mathbf{p} = \boldsymbol{\xi} \times [\mathbf{E} + \boldsymbol{\xi} \times \mathbf{H}], \tag{3.1a}$$

$$\mathbf{q} = \boldsymbol{\xi} \times [\mathbf{E} - \boldsymbol{\xi} \times \mathbf{H}]. \tag{3.1b}$$

These will be supplemented by the components of the fields along $\boldsymbol{\xi}$

$$h = \boldsymbol{\xi} \cdot \mathbf{H}, \tag{3.2a}$$

$$e = \boldsymbol{\xi} \cdot \mathbf{E}. \tag{3.2b}$$

Taking, e.g., $\boldsymbol{\xi}$ parallel to x, one can verify that the two components of $\mathbf{p}$ are eigenvectors of A_1 with eigenvalue $+1$, while the components of $\mathbf{q}$ are eigenvectors with eigenvalue -1. Note that there are still only six unknowns, because $\mathbf{p} \cdot \boldsymbol{\xi} = \mathbf{q} \cdot \boldsymbol{\xi} = 0$.

The focus of this development is to derive boundary conditions suitable for application in cell-based numerical simulations, where one is free to take each cell at the outer boundary to have a simple shape with

a single, flat facet at the boundary. In that case, the direction of $\boldsymbol{\xi}$ is constant on this boundary, and Maxwell's equations take the form:

$$\partial\mathbf{p}/\partial t - \partial\mathbf{p}/\partial x - (\boldsymbol{\eta}\partial/\partial y + \boldsymbol{\zeta}\partial/\partial z)h + \boldsymbol{\xi}\times(\boldsymbol{\eta}\partial/\partial y + \boldsymbol{\zeta}\partial/\partial z)e = 0, \tag{3.3}$$

$$\partial\mathbf{q}/\partial t + \partial\mathbf{q}/\partial x - (\boldsymbol{\eta}\partial/\partial y + \boldsymbol{\zeta}\partial/\partial z)h - \boldsymbol{\xi}\times(\boldsymbol{\eta}\partial/\partial y + \boldsymbol{\zeta}\partial/\partial z)e = 0, \tag{3.4}$$

$$\partial h/\partial t - \frac{1}{2}\partial[\boldsymbol{\eta}\cdot(\mathbf{p}+\mathbf{q})]/\partial y - \frac{1}{2}\partial[\boldsymbol{\zeta}\cdot(\mathbf{p}+\mathbf{q})]/\partial z = 0, \tag{3.5}$$

$$\partial e/\partial t + \frac{1}{2}\partial[\boldsymbol{\zeta}\cdot(\mathbf{p}-\mathbf{q})]/\partial y - \frac{1}{2}\partial[\boldsymbol{\eta}\cdot(\mathbf{p}-\mathbf{q})]/\partial z = 0, \tag{3.6}$$

where $\boldsymbol{\eta}$ and $\boldsymbol{\zeta}$ are unit vectors along the y and z axes, respectively, in a right-handed Cartesian system ($\boldsymbol{\xi}\times\boldsymbol{\eta} = \boldsymbol{\zeta}$). In addition, one imposes the divergence conditions $\nabla\cdot\mathbf{H} = 0 = \nabla\cdot\mathbf{E}$ within the cell, which can be written in terms of the new variables as

$$\partial h/\partial x - \frac{1}{2}\partial[\boldsymbol{\eta}\cdot(\mathbf{p}-\mathbf{q})]/\partial y - \frac{1}{2}\partial[\boldsymbol{\zeta}\cdot(\mathbf{p}-\mathbf{q})]/\partial z = 0, \tag{3.7}$$

$$\partial e/\partial x + \frac{1}{2}\partial[\boldsymbol{\zeta}\cdot(\mathbf{p}+\mathbf{q})]/\partial y - \frac{1}{2}\partial[\boldsymbol{\eta}\cdot(\mathbf{p}+\mathbf{q})]/\partial z = 0. \tag{3.8}$$

The fact that $\partial h/\partial x$ and $\partial e/\partial x$ do not appear in Eqs. (3.3)–(3.6) is a reflection of the singularity of the matrix A_1. To remove this singularity, we shall modify Eqs. (3.5) and (3.6) by subtracting the divergence conditions, each multiplied by a scalar constant ε:

$$\partial h/\partial t - \varepsilon\partial h/\partial x - \frac{1}{2}\boldsymbol{\eta}\cdot\partial[(1-\varepsilon)\mathbf{p} + (1+\varepsilon)\mathbf{q}]/\partial y - \frac{1}{2}\boldsymbol{\zeta}\cdot\partial[(1-\varepsilon)\mathbf{p} + (1+\varepsilon)\mathbf{q}]/\partial z = 0, \tag{3.9}$$

$$\partial e/\partial t - \varepsilon\partial e/\partial x + \frac{1}{2}\boldsymbol{\zeta}\cdot\partial[(1-\varepsilon)\mathbf{p} - (1+\varepsilon)\mathbf{q}]/\partial y - \frac{1}{2}\boldsymbol{\eta}\cdot\partial[(1-\varepsilon)\mathbf{p} - (1+\varepsilon)\mathbf{q}]/\partial z = 0. \tag{3.10}$$

These two equations now represent a weaker set of requirements than (3.5)–(3.8), admitting solutions that are unphysical, as well as including all the solutions of the original set. The matrix coefficient of $\partial/\partial x$ in this new set of Eqs. (3.3), (3.4), (3.9) and (3.10) is nonsingular so long as $\varepsilon \neq 0$, the two zero eigenvalues being replaced by ε, while the other four eigenvalues are unchanged at ± 1. Gustafsson [18] used a similar modification in treating the scalar wave equation as a first-order system, where a zero eigenvalue also appears.

One can now employ the same procedure as Engquist and Majda [1], Fourier transforming these equations with respect to y, z, and t, and solving the resultant set for $\partial u/\partial x$, where u is now the column vector $(\mathbf{p},\mathbf{q},h,e)^{\mathrm{T}}$:

$$\partial\mathbf{p}/\partial x = \mathrm{i}\omega\mathbf{p} - \mathrm{i}\mathbf{k}h + (\boldsymbol{\xi}\times\mathrm{i}\mathbf{k})e, \tag{3.11}$$

$$\partial\mathbf{q}/\partial x = -\mathrm{i}\omega\mathbf{q} + \mathrm{i}\mathbf{k}h + (\boldsymbol{\xi}\times\mathrm{i}\mathbf{k})e, \tag{3.12}$$

$$\partial h/\partial x = \gamma\mathrm{i}\omega h + \frac{1}{2}\mathrm{i}\mathbf{k}\cdot[(1-\gamma)\mathbf{p} - (1+\gamma)\mathbf{q}], \tag{3.13}$$

$$\partial e/\partial x = \gamma\mathrm{i}\omega e - \frac{1}{2}(\boldsymbol{\xi}\times i\mathbf{k})\cdot[(1-\gamma)\mathbf{p} + (1+\gamma)\mathbf{q}]. \tag{3.14}$$

Here $\partial/\partial t$ has been replaced by $\mathrm{i}\omega$, $\partial/\partial y$ by $\boldsymbol{\eta}\cdot\mathrm{i}\mathbf{k}$, and $\partial/\partial z$ by $\boldsymbol{\zeta}\cdot\mathrm{i}\mathbf{k}$. The vector $\mathbf{k}$ lies in the plane perpendicular to $\boldsymbol{\xi}$; it will be useful to define the unit vector parallel to $\mathbf{k}$ as $\boldsymbol{\alpha}$ and the unit vector $\boldsymbol{\xi}\times\boldsymbol{\alpha}$ as $\boldsymbol{\beta}$. We have also put $\gamma = 1/\varepsilon$ for convenience.

Taking scalar products of (3.11) and (3.12) with $\boldsymbol{\alpha}$ and $\boldsymbol{\beta}$, one finds that Eqs. (3.11)–(3.14) can be separated into two simpler sets of three. Define the three-component column vector $\underline{aw} = (\boldsymbol{\alpha}\cdot\mathbf{p}, \boldsymbol{\alpha}\cdot\mathbf{q}, h)^{\mathrm{T}}$, and the column vector $\underline{bw} = (\boldsymbol{\beta}\cdot\mathbf{p}, \boldsymbol{\beta}\cdot\mathbf{q}, e)^{\mathrm{T}}$. Then the two sets can be written as

$$\partial(\underline{aw})/\partial x = \mathrm{i}A\underline{aw}, \tag{3.15}$$

$$\partial(\underline{bw})/\partial x = \mathrm{i}B\underline{bw}, \tag{3.16}$$

where the matrices A and B are given by

$$A = \begin{matrix} \omega & 0 & -k \\ 0 & -\omega & k \\ \frac{1}{2}k(1-\gamma) & -\frac{1}{2}k(1+\gamma) & \gamma\omega \end{matrix} \tag{3.17a}$$

and

$$B = \begin{matrix} \omega & 0 & k \\ 0 & -\omega & k \\ -\frac{1}{2}k(1-\gamma) & -\frac{1}{2}k(1+\gamma) & \gamma\omega \end{matrix}. \tag{3.17b}$$

The eigenvalues for these two matrices are identical, being given by

$$\lambda_1 = \sqrt{(\omega^2 - k^2)}, \tag{3.18a}$$

$$\lambda_2 = -\sqrt{(\omega^2 - k^2)}, \tag{3.18b}$$

$$\lambda_3 = \gamma\omega. \tag{3.18c}$$

To diagonalize the two systems of equations, one needs the left eigenvectors for each matrix. In both cases, the elements of these eigenvectors can be written simply in terms of the following ratios:

$$g = (1-\gamma)/(1+\gamma), \tag{3.19a}$$

$$r = (\omega - \lambda_1)/(\omega + \lambda_1), \tag{3.19b}$$

$$d = -2(\omega - \lambda_1)/k(1-\gamma). \tag{3.19c}$$

Using this notation, the left eigenvectors for A are

$$\underline{\ell}_1 = [1, r/g, d], \tag{3.20a}$$

$$\underline{\ell}_2 = [rg, 1, dg], \tag{3.20b}$$

$$\underline{\ell}_3 = [-k/2\omega, -k/2\omega, 1], \tag{3.20c}$$

while those for B are

$$\underline{\mu}_1 = [1, -r/g, -d], \tag{3.21a}$$

$$\underline{\mu}_2 = [-rg, 1, dg], \tag{3.21b}$$

$$\underline{\mu}_3 = [k/2\omega, -k/2\omega, 1]. \tag{3.21c}$$

Using these eigenvectors, one can show, e.g., that

$$\partial(\ell_1 \cdot \underline{aw})/\partial x = \mathrm{i}\lambda_1(\ell_1 \cdot \underline{aw}), \tag{3.22a}$$

$$\partial(\underline{\mu}_1 \cdot \underline{bw})/\partial x = \mathrm{i}\lambda_1(\underline{\mu}_1 \cdot \underline{bw}). \tag{3.22b}$$

Now, following the analysis by Engquist and Majda [1], these two linear combinations, $(\ell_1 \cdot \underline{aw})$ and $(\underline{\mu}_1 \cdot \underline{bw})$, represent the incoming waves; requiring that they vanish at the outer boundary gives the theoretical nonlocal absorbing boundary conditions:

$$(\boldsymbol{\alpha} \cdot \mathbf{p}) + r/g(\boldsymbol{\alpha} \cdot \mathbf{q}) + \mathrm{d}h = 0, \tag{3.23}$$

$$(\boldsymbol{\beta} \cdot \mathbf{p}) - r/g(\boldsymbol{\beta} \cdot \mathbf{q}) - \mathrm{d}e = 0. \tag{3.24}$$

These conditions apply, of course, to the set of equations that incorporate the weaker relations (3.9) and (3.10), rather than (3.5) and (3.6). However, these weaker relations can be made to approach (3.5) and (3.6) in the limit of large γ, at least in the sense of singular perturbation. And in this limit, the conditions (3.23) and (3.24) remain well-defined, approaching the form:

$$(\boldsymbol{\alpha} \cdot \mathbf{p}) - r(\boldsymbol{\alpha} \cdot \mathbf{q}) = 0, \tag{3.25}$$

$$(\boldsymbol{\beta} \cdot \mathbf{p}) + r(\boldsymbol{\beta} \cdot \mathbf{q}) = 0. \tag{3.26}$$

Substituting for $(\boldsymbol{\alpha} \cdot \mathbf{q})$ in terms of $(\boldsymbol{\alpha} \cdot \mathbf{p})$ and h from the Fourier transform of Eq. (3.5), and similarly for $(\boldsymbol{\beta} \cdot \mathbf{q})$ in terms of $(\boldsymbol{\beta} \cdot \mathbf{p})$ and e from the transform of Eq. (3.6), one finds after some algebra:

$$(\boldsymbol{\alpha} \cdot \mathbf{p}) = k^{-1}(\omega - \lambda_1)h, \tag{3.27}$$

$$(\boldsymbol{\beta} \cdot \mathbf{p}) = -k^{-1}(\omega - \lambda_1)e. \tag{3.28}$$

Recalling that $\boldsymbol{\alpha}$ and $\boldsymbol{\beta}$ are orthogonal unit vectors in the plane perpendicular to $\boldsymbol{\xi}$, one can combine these two scalar relations to give

$$\mathbf{p} = -k^{-2}(\mathrm{i}\omega - \mathrm{i}\lambda_1)[\mathrm{i}\mathbf{k}h - (\boldsymbol{\xi} \times \mathrm{i}\mathbf{k})e], \tag{3.29}$$

where the imaginary unit has been restored to the expression in order make the mapping back to derivatives more transparent. The theoretical perfectly absorbing nonlocal boundary condition can thus be written in terms of pseudo-differential operators as

$$(\partial^2/\partial y^2 + \partial^2\partial z^2)\mathbf{p} = -\{\partial/\partial t - \sqrt{[\partial^2/\partial t^2 - (\partial^2/\partial y^2 + \partial^2/\partial z^2)]}\}[\boldsymbol{\xi} \times (\boldsymbol{\xi} \times \nabla)h + (\boldsymbol{\xi} \times \nabla)e]. \tag{3.30}$$

Since the operator $(\partial^2/\partial y^2 + \partial^2\partial z^2)$ is just the divergence in the tangent plane at the outer boundary, it will be denoted as ∇_t^2 in the remainder of this paper.

A result equivalent to Eq. (3.30) has been obtained by Hagstrom [10] as part of a general investigation of absorbing boundary conditions. In our notation, his form of the absorbing boundary condition reads

$$2\partial\mathbf{p}/\partial t - \{\partial/\partial t - \sqrt{[\partial^2/\partial t^2 - (\partial^2/\partial y^2 + \partial^2/\partial z^2)]}\}\mathbf{p} + \boldsymbol{\xi} \times (\boldsymbol{\xi} \times \nabla)h + (\boldsymbol{\xi} \times \nabla)e = 0. \tag{3.31}$$

The equivalence follows in a straightforward way by making use of the fact that $\mathbf{p}$ satisfies the scalar wave equation, $\nabla_t^2\mathbf{p} = (\partial^2/\partial t^2 - \partial^2/\partial x^2)\mathbf{p} = (\partial/\partial t - \partial/\partial x)(\partial/\partial t + \partial/\partial x)\mathbf{p}$, and noting from Eq. (3.3) that $\boldsymbol{\xi} \times (\boldsymbol{\xi} \times \nabla)h + (\boldsymbol{\xi} \times \nabla)e = -(\partial/\partial t - \partial/\partial x)\mathbf{p}$.

4. The boundary conditions

4.1. The first three ABC's

To obtain approximate local absorbing boundary conditions from any of these forms, the eigenvalue λ_1 can be approximated by local derivative operations, as in the Engquist–Majda development [1]. Expanding λ_1 for k small compared to ω in (3.29), one finds to lowest order $\lambda_1 \approx \omega$, which gives

$$\mathbf{p} = 0 \quad \text{(first approximation)}. \tag{4.1}$$

This vanishing of the incoming characteristic combination of $\mathbf{E}$ and $\mathbf{H}$ is the boundary condition that has been implemented in most finite-volume simulations of Maxwell's equations [11]. It is a natural condition to apply when the fields are taken as constant inside the finite-volume cell. The magnitude of its plane wave reflection coefficient is $(1 - \cos(\theta))/(1 + \cos(\theta))$.

If one keeps the first nonvanishing term in k^2 in the expansion of λ_1, namely putting $\lambda_1 \approx \omega - k^2/2\omega$, one obtains

$$\mathrm{i}\omega\mathbf{p} = \frac{1}{2}[\mathrm{i}\mathbf{k}h - (\boldsymbol{\xi} \times \mathrm{i}\mathbf{k})e] \quad \text{(second approximation)}. \tag{4.2}$$

In terms of derivatives, the second approximation takes the form

$$\partial\mathbf{p}/\partial t = -\frac{1}{2}[\boldsymbol{\xi} \times (\boldsymbol{\xi} \times \nabla)h + (\boldsymbol{\xi} \times \nabla)e], \tag{4.3}$$

which gives a reflection coefficient of magnitude $(1 - \cos(\theta))^2/(1 + \cos\theta)^2$ for both TE ($\boldsymbol{\xi} \cdot \mathbf{E} = 0$) and TM ($\boldsymbol{\xi} \cdot \mathbf{H} = 0$) waves. It reduces exactly to the Engquist–Majda scalar-wave second approximation [1] in both cases.

To obtain the third approximation for the vector system, the root λ_1 must be expressed to higher order in the ratio k/ω. As Engquist and Majda note in [1], simple Taylor expansion of the square root does not lead to a stable scheme. However, one can make use of their Pade' approximation

$$\sqrt{[1 - (k/\omega)^2]} \approx 1 - (k/\omega)^2/[2 - \frac{1}{2}(k/\omega)^2] + \mathrm{O}((\kappa/\omega)^6) \tag{4.4}$$

to construct a third vector absorbing boundary condition. This gives

$$\omega^2[2 - \frac{1}{2}(k/\omega)^2]\mathbf{p} = -\mathrm{i}(\omega)[\mathrm{i}\mathbf{k}h - (\boldsymbol{\xi} \times \mathrm{i}\mathbf{k})e], \tag{4.5}$$

which can be mapped to the differential equation

$$2\partial^2\mathbf{p}/\partial t^2 - \frac{1}{2}\nabla_t^2\mathbf{p} = -\partial/\partial t[\boldsymbol{\xi} \times (\boldsymbol{\xi} \times \nabla)h + (\boldsymbol{\xi} \times \nabla)e]. \tag{4.6}$$

Again, this agrees with the Engquist–Majda result [1]. One can recast (4.6) as

$$\partial/\partial t\{\partial\mathbf{p}/\partial t + \frac{1}{2}[\boldsymbol{\xi} \times \boldsymbol{\xi} \times \nabla)h + (\boldsymbol{\xi} \times \nabla)e]\} = \frac{1}{4}\nabla_t^2\mathbf{p}, \tag{4.7}$$

which extends condition (4.3) in a natural way.

4.2. The infinite sequence of ABC's

The form of the three conditions (4.1), (4.3) and (4.7) is suggestive of a pattern that can be extended to arbitrary order. One can regard the second-order Pade' approximation to $\sqrt{(1+x)}$ as one step in the infinite ladder of approximations generated by the continued-fraction expansion of the square root: $\sqrt{(1+x)} = 1 + x/[2 + x/(2 + \cdots)]$.

At the mth stage, this fraction can be rationalized to give

$$\sqrt{(1+x)} = 1 + \frac{1}{2}x(C_m/C_{m+1}) + \mathrm{O}(|x|^{m+1}), \tag{4.8}$$

where

$$C_m = C_{m-1} + \frac{1}{4}xC_{m-2}, \tag{4.9}$$

and

$$C_0 = 0, \quad C_1 = 1. \tag{4.10}$$

The absorbing boundary condition generated at this stage can be written as

$$\omega C_{m+1}\mathbf{p} = \frac{1}{2}C_m[\mathbf{k}h - (\boldsymbol{\xi} \times \mathbf{k})e], \tag{4.11}$$

and transformed into derivatives as before, putting $x = -(k/\omega)^2$.

The solution to the recursion relation (4.9) can be written in closed form as a polynomial in x. Using the symbol $(m|j)$ for the binomial coefficient "m choose j" $= m!/j!\,(m-j)!$, this polynomial takes the form

$$C_m(x) = \sum (m-j-1|j)\left(\frac{1}{4}x\right)^j, \tag{4.12}$$

where the sum runs from $j = 0$ to $j = \frac{1}{2}(m-1)$ for m odd and to $(\frac{1}{2}m) - 1$ for m even.

With the aid of this expression for C_m, the differential equation corresponding to Eq. (4.11) can be written down explicitly. Denoting

$$\mathbf{s} = \frac{1}{2}[\boldsymbol{\xi} \times (\boldsymbol{\xi} \times \nabla)(\boldsymbol{\xi} \cdot \mathbf{H}) + (\boldsymbol{\xi} \times \nabla)(\boldsymbol{\xi} \cdot \mathbf{E})], \tag{4.13}$$

this differential equation takes the form

$$\sum \left[-\frac{1}{4}\nabla_t^2\right]^j \left\{(m-j|j)(\partial/\partial t)^{m-2j}\mathbf{p} + (m-j-1|j)(\partial/\partial t)^{m-2j-1}\mathbf{s}\right\} = 0. \qquad (\mathrm{ABC})_m$$

Here the condition $\mathbf{p} = 0$ has been designated as $(\mathrm{ABC})_0$, and we have used the fact that $(m-j|j)$ vanishes for $\frac{1}{2}m < j < m$ to combine the two summations with a single upper limit $[\frac{1}{2}m]$, where $[x]$ denotes the largest integer in x.

Engquist and Majda in [2] used a very similar technique to the above to construct an infinite sequence of boundary conditions for the scalar wave equation, and several subsequent authors have explored alternative sequences chosen to minimize scalar-wave reflection according to different criteria. Higdon [12,13], Halpern and Trefethen [14], and Zhang [15] provide detailed examples of this kind. It appears that the explicit form of the conditions above for Maxwell's equations is exhibited here for the first time.

Recently, Ditkowski and Gottlieb [16] have derived a particularly simple form for the mth-order absorbing boundary condition for Maxwell's equations in terms of normal derivatives at the boundary. In our notation their result is

$$(\partial/\partial t + \partial/\partial x)^m\mathbf{p} = 0, \qquad (\mathrm{ABC}^*)_m$$

a form that only differs from Higdon's product condition for minimizing reflection near normal incidence [12] by the replacement of u, the scalar wave unknown, by $\mathbf{p}$. Its equivalence to the condition above is easily established by applying $(\partial/\partial t + \partial/\partial x)$ to the left-hand side of $(\mathrm{ABC})_m$ and using the recursion relation (4.9) to rewrite the term involving $\mathbf{s}$. This procedure yields $2(\mathrm{ABC})_{m+1}$. It is straightforward to show from this expression that the plane wave reflection coefficient for either component of $\mathbf{p}$ has magnitude $[(1-\cos(\theta))/(1+\cos(\theta))]^{m+1}$ (see, e.g. [13]).

As written above, each $(\mathrm{ABC})_m$ is a an mth-order partial differential equation to be solved on the boundary, with a lowest-order time derivative term that depends upon whether m is odd or even. This lowest-order term $\mathbf{S}_m$ involves only tangential derivatives of field quantities at the outer boundary. It is given by

$$\mathbf{S}_m = \left[-\frac{1}{4}\nabla_t^2\right]^{(m-1)/2}\mathbf{s} \tag{4.14}$$

for m odd, and by

$$\mathbf{S}_m = \left[-\frac{1}{4}\nabla_t^2\right]^{m/2}\mathbf{p} \tag{4.15}$$

for m even. Compare (4.3) and (4.7) for $m = 1$ and 2, respectively.

5. Well-posedness

A necessary condition for the stability of any numerical time integration scheme for a constant-coefficient hyperbolic system with boundary condition B is that there be no plane wave solutions bounded in space and satisfying B that grow exponentially in time. The form of such a growing solution to Maxwell's equations at a plane boundary where the outward normal points along the positive x axis is

$$w(s,\mathbf{k}) = w_0 \exp[\mathrm{i}\mathbf{k}\cdot\mathbf{r} + x\sqrt{(s^2+k^2)} + st], \tag{5.1}$$

where $\mathbf{k}$ is a vector in the y–z plane and $\mathrm{Re}\, s > 0$.

Substituting (5.1) into Maxwell's equations, one finds that the vectors $\mathbf{p}$ and $\mathbf{q}$ can be expressed in terms of the scalars h and e as

$$\mathbf{p} = -[s + \sqrt{(s^2+k^2)}][\mathrm{i}\mathbf{k}h - (\boldsymbol{\xi}\times i\mathbf{k})e]/k^2, \tag{5.2}$$

$$\mathbf{q} = -[s - \sqrt{(s^2+k^2)}][\mathrm{i}\mathbf{k}h + (\boldsymbol{\xi}\times i\mathbf{k})e]/k^2. \tag{5.3}$$

The mth order boundary condition, by virtue of (4.11), takes a similar form

$$sC_{m+1}(x)\mathbf{p} = \frac{1}{2}C_m(x)[\mathrm{i}\mathbf{k}h - (\boldsymbol{\xi}\times \mathrm{i}\mathbf{k})e], \tag{5.4}$$

where we have put $x = (k/s)^2$. Combining (5.2) and (5.4), one sees that both the vector component of the condition along $\mathbf{k}$ and the component along $(\boldsymbol{\xi}\times\mathbf{k})$ result in the same scalar condition, which can be written in the form

$$C_{m+1}(x)[1 + \sqrt{(1+x)}] + \frac{1}{2}xC_m(x) = 0, \tag{5.5}$$

or more suggestively as

$$\sqrt{(1+x)} = -\left[1 + \frac{1}{2}xC_m(x)/C_{m+1}(x)\right]. \tag{5.6}$$

The bracketed expression on the right-hand side of (5.6) will be recognized from Eq. (4.8) as the mth approximation to $\sqrt{(1+x)}$ itself.

If one squares both sides of (4.8) and clears the denominator, the result after using the recursion relation (4.9) to simplify is

$$x[C_{m+1}(x)]^2 - xC_m(x)C_{m+2}(x) = \mathrm{O}(|x|^{m+1}). \tag{5.7}$$

Both products on the left are finite polynomials in x, and the highest-order term is found to be $\pm x\,(x/4)^m$, depending upon whether m is odd or even. The only way that their combined order can be bounded by $|x^{m+1}|$ as $x \to 0$ is for the coefficient of every power of x smaller than $m+1$ to vanish. That is, we have proved indirectly the relation

$$[C_{m+1}(x)]^2 = C_m(x)C_{m+2}(x) + (-x/4)^m. \tag{5.8}$$

Applying this result to the square of (5.6), one then arrives at the condition

$$x^{m+1} = 0, \tag{5.9}$$

which can be satisfied only by putting $k^2 = 0$. The conditions (5.4) then reduce to

$$2s^2 = 0, \tag{5.10}$$

showing that there is no root of (5.5) with $\mathrm{Re}\, s > 0$.

Each $(\mathrm{ABC})_m$, when written as a function of s and k, is continuous. Consequently, on the surface of the sphere $|s^2| + k^2 = 1$, it has a nonzero minimum (its only zero is isolated at the origin). Kreiss [17] showed that the existence of such a minimum is sufficient to establish bounds on the solution over the whole domain that hold over any finite time interval. Engquist and Majda in [2] develop explicit bounds of this type for solutions of the scalar wave equation, which would apply to $\mathbf{p}$ when any of our absorbing boundary conditions are used to close the system of equations.

Gustafsson [18] and Higdon [12] have pointed out that the direct implementation of derivative boundary conditions, such as our $(\mathrm{ABC})_m$ for $m \neq 0$ entails the appearance of a weak instability in the solution, and Trefethen [19] has characterized the types of instability that can arise. The vanishing of B at $s = 0$, which is recognized as a generalized eigenvalue of the problem, is found to imply that nonzero data at the outer boundary can lead to polynomial growth in the interior. Ditkowski and Gottlieb [16] construct an explicit example of this behavior for their form of the absorbing boundary conditions. However, in [18] Gustafsson also shows that implementing an integrated form of the boundary conditions can ameliorate the effect of the instability. This is what we have chosen to do in the following section.

6. Implementation

The motivation for our development of high-order absorbing boundary conditions is to preserve the inherent solution accuracy of integration schemes that employ a high-order representation for the unknowns inside each computational cell. In this section a particular integration scheme of this type due to Cockburn and Shu [3], the Runge–Kutta discontinuous Galerkin (RKDG) scheme, is adopted to investigate how these boundary conditions may function in practice.

Consider now an unstructured grid covering some finite, convex part of an infinite domain in which Maxwell's equations (2.1a)–(2.2b) are satisfied, enclosing a scatterer or source of electromagnetic radiation. Choose the grid cells that terminate the grid at its outer boundary each to have a single, flat facet on this boundary, all of their other facets being interior to the grid. On this outer facet, each of the $(\mathrm{ABC})_m$ other than $m = 0$ is a partial differential equation relating tangential derivatives of $\mathbf{p}$ and $\mathbf{s}$ to their time derivatives.

When highorder spatial representations for the unknowns are available in each grid cell, one can implement any of the absorbing boundary conditions using only information local to the boundary cell in determining the incoming wave data at the cell boundary. At lowest order, this amounts to requiring $\mathbf{p} = \boldsymbol{\xi} \times [\mathbf{E} + \boldsymbol{\xi} \times \mathbf{H}] = 0$ on each boundary facet, where $\boldsymbol{\xi}$ is the unit normal on that facet. The tangential fields on the facet in this case are then given from Eq. (3.1a), (3.1b) as

$$\boldsymbol{\xi} \times \mathbf{E} = \frac{1}{2}(\mathbf{p} + \mathbf{q}^-) = \frac{1}{2}\boldsymbol{\xi} \times [\mathbf{E}^- - \boldsymbol{\xi} \times \mathbf{H}^-], \tag{6.1a}$$

$$\boldsymbol{\xi} \times \boldsymbol{\xi} \times \mathbf{H} = \frac{1}{2}(\mathbf{p} - \mathbf{q}^-) = -\frac{1}{2}\boldsymbol{\xi} \times [\mathbf{E}^- - \boldsymbol{\xi} \times \mathbf{H}^-], \tag{6.1b}$$

where the minus superscript indicates that the field components are those determined by the spatial representation inside the cell.

In the same spirit, for an order m absorbing boundary condition, one can implement the partial differential equation as a set of first-order ordinary differential equations for the local variables $\{\mathbf{P}_k(t); k = 0 \text{ to } m-1\}$ satisfying

$$\mathrm{d}\mathbf{P}_{m-1-k}/\mathrm{d}t + \left(\left[\frac{1}{2}(m+k)\right]|k\right)\mathbf{S}^-_{m-k} = \mathbf{P}_{m-k}, \tag{6.2}$$

with $\mathbf{P}_m = 0$ and $\mathbf{P}_0 = \mathbf{p}$, and with initial conditions $\mathbf{P}_k(0) = 0$. As before, $[x]$ denotes the largest integer in x. Here the source terms $\mathbf{S}^-_{m-k}$ are just those given in Eqs. (4.14) and (4.15), evaluated using the spatial representation internal to the particular boundary cell. The value of $\mathbf{p}$ derived from these equations then determines the tangential fields on the facet from (6.1a), (6.1b). The set of $\mathbf{P}_k$ governed by this process can be regarded as a particular form of the "auxiliary functions" defined by Hagstrom [10] and others [15,20] in their implementations of higher order absorbing boundary conditions. Most recently, Givoli and Neta [21] have carried out such an implementation for semi-infinite rectangular waveguides, starting from the Higdon product conditions [12,13].

The magnitude of the error incurred by the simplifications inherent in this local implementation for a faceted convex boundary appears difficult to estimate analytically. However, one can gain some insight by applying the implementation to unit problems that have a known or calculable answer.

As a test case for our approach, we have selected the pulsed electric dipole example of Grote and Keller [20], in which the gridded region is a spherical shell, and the dipole is placed inside the interior boundary of the shell. These authors used an expansion of the solution in spherical harmonics to deduce an exact absorbing boundary condition at the spherical outer boundary. For each harmonic (n, m), this condition requires the solution of a system of first-order ordinary differential equations for $2n$ auxiliary functions of time. An approximate absorbing boundary condition is obtained by truncating the infinite sum over harmonics at a finite order.

For our numerical test the spherical shell has been gridded using nine regular layers of hexahedrons, as illustrated in Fig. 1. The interior of the shell is composed of six identical sections, each containing $9 \times 15 \times 15$ hexahedrons. The exterior face of each hexahedron on the outer boundary is flat, while the innermost face of each hexahedron on the inner boundary is curved to match a spherical surface up to second order.

To facilitate a comparison with Grote and Keller's results [20], the dimensions of the shell have been taken the same as theirs: an inner radius of 50 cm and an outer radius of one meter. The location of the dipole source (40 cm from the center of the sphere) and the Gaussian shape of its pulse are also the same, although our pulse width is a few percent narrower. Specifically, we take the Hertz vector $\boldsymbol{\Pi}$ for the dipole to be given by (see Fig. 2)

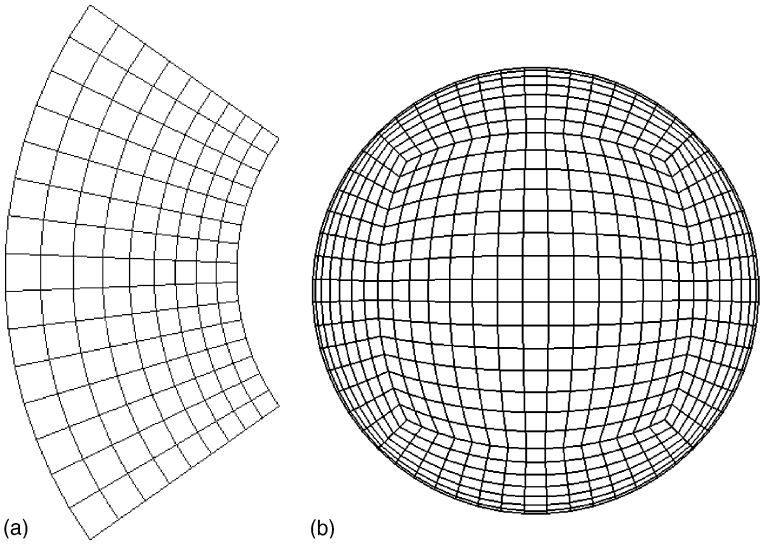

Fig. 1. Hexahedral grid for the spherical shell: (a) radial cross-section from one of six identical sectors; (b) grid lines on the inner-spherical surface.

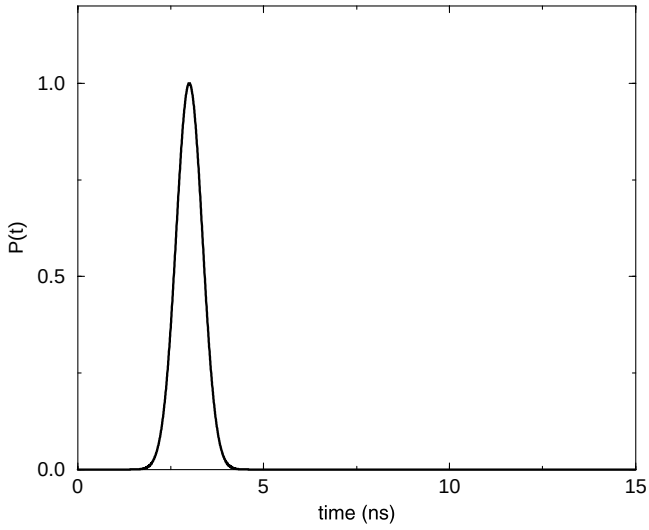

Fig. 2. Shape of the transient dipole moment used to derive incident electric and magnetic fields at the inner spherical boundary: $\exp -(t-t_0)^2/\sigma^2$.

$$\mathbf{\Pi}(\mathbf{r}) = (\mathbf{z}/d)\exp -(t - d/c - t_0)^2/\sigma^2, \tag{6.3}$$

with $\sigma = 0.5$ ns and $t_0 = 3$ ns, where $\mathbf{z}$ is a unit vector along the line connecting the dipole to the center of the sphere and d is the distance from the dipole to the field point at $\mathbf{r}$. Expressions for the corresponding electric and magnetic fields can be found in [22].

Our implementation of the RKDG method [3] for integrating Maxwell's equations has been described elsewhere [23]. Essentially, each field component in each cell is expanded in general polynomials of the

spatial coordinates up to some defined order, and the coefficients in these expansions are taken to be time dependent. A Riemann problem is solved at each cell interface to determine the tangential fields on the interface in terms of the coefficients on either side. By an application of Green's theorem, integrating these interface fields against each expansion polynomial around the whole cell surface yields a set of ordinary differential equations in time for the coefficients. These equations are then integrated forward in time using a standard fourth-order Runge–Kutta scheme.

In the present implementation of the absorbing boundary conditions, the interface fields on the outer boundary involve only the coefficients of the parent cell and the local value of **p**. The ordinary differential equations (6.2) determining **p** are integrated using the same Runge–Kutta scheme with the same time step as that for the interior cells. Only the values of $\mathbf{P}_k$ ($k = 0$ to $m - 1$) at each quadrature point selected for the surface integration are retained as new time-dependent unknowns.

For the purposes of this test, the spatial expansion in each cell was truncated at terms quadratic in the coordinates. This gave acceptable accuracy in propagating the dipolar fields throughout the spherical shell and provided a convenient platform for investigating the efficacy of applying the first three absorbing boundary conditions.

Figs. 3–5 show the history of the magnetic field at each of three cell-centroid locations inside the spherical shell (chosen close to those used in [20]). It is not our intention to report on an extensive investigation of the factors affecting error behavior in the current paper. Rather, we seek only to illustrate that the qualitative trends with the order of the absorbing boundary condition are consistent with expectations.

At all three locations the reflected error is about the same magnitude for a given ABC, while the exact signal decreases by a factor of around 10 from $\theta = 42°$ to $\theta = 167°$. The progressively later time of arrival of the reflected error as one moves from $\theta = 42°$ to $\theta = 167°$ indicates that the strongest reflected signal is originating near $\theta = 30°$, as one expects from the shape of the radiation pattern for this vertical dipole at $z = 40$ cm.

Our results for $(\mathrm{ABC})_0$ appear quite similar to those of Grote and Keller [20] for the first Peterson condition (which puts $\partial\mathbf{p}/\partial t = 0$ at the outer boundary). The decreases in maximum observed error upon applying $(\mathrm{ABC})_1$ and $(\mathrm{ABC})_2$ are significant, but they vary with position and do not follow simply from

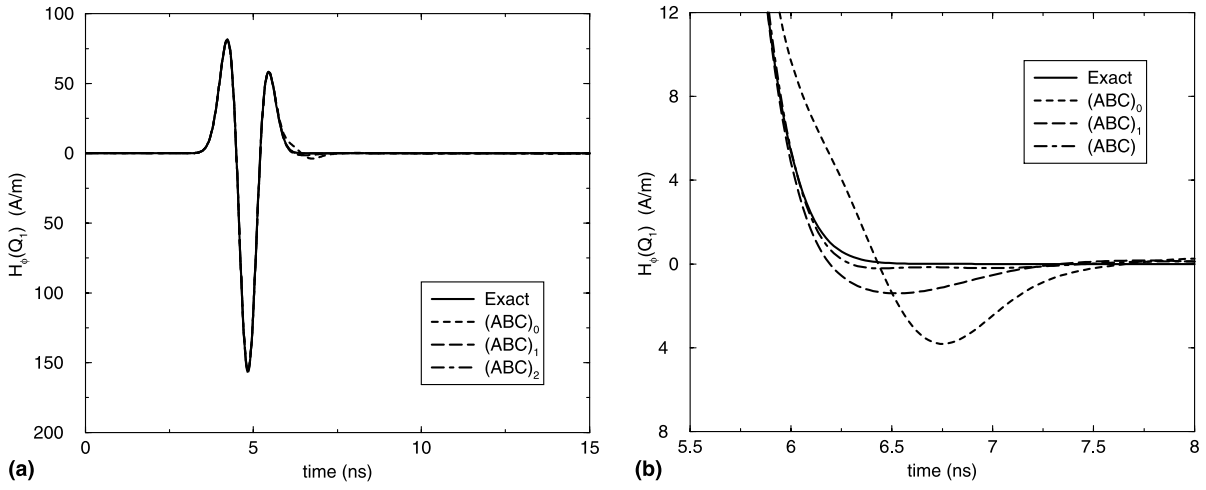

Fig. 3. Azimuthal magnetic field intensity at the point $(r, \theta) = (0.768, 42.4°)$ for the first three absorbing boundary conditions. The dipole source is located at $(0.4, 0)$. Exact solution is shown as a solid line, $(\mathrm{ABC})_0$ as lightly dashed, $(\mathrm{ABC})_1$ as heavily dashed, and $(\mathrm{ABC})_2$ as dot-dashed lines: (a) first 15 ns; (b) close-up showing the reflected error. Radial distances are quoted in meters.

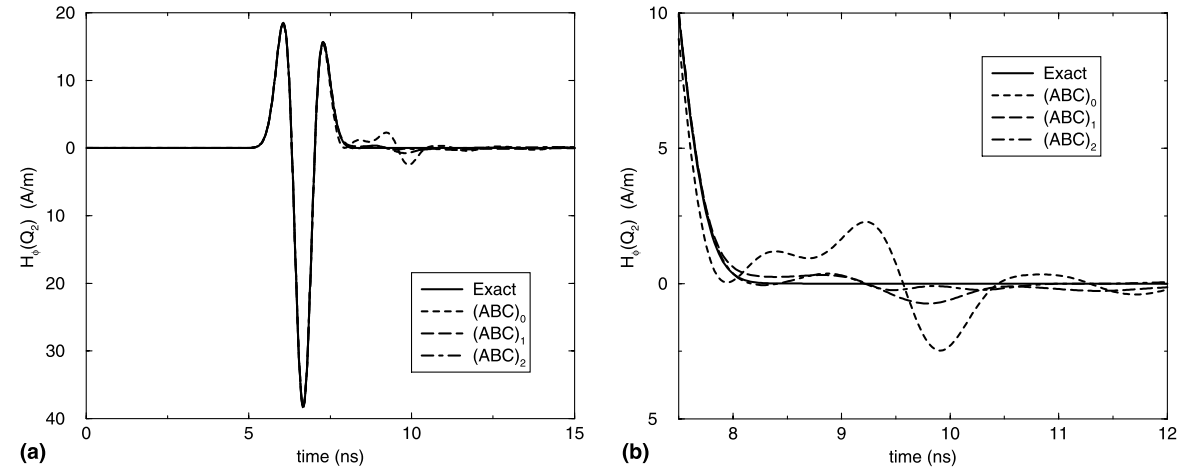

Fig. 4. Azimuthal magnetic field intensity at the point $(r, \theta) = (0.768, 137.6°)$ for the first three absorbing boundary conditions. Conventions are the same as in Fig. 3.

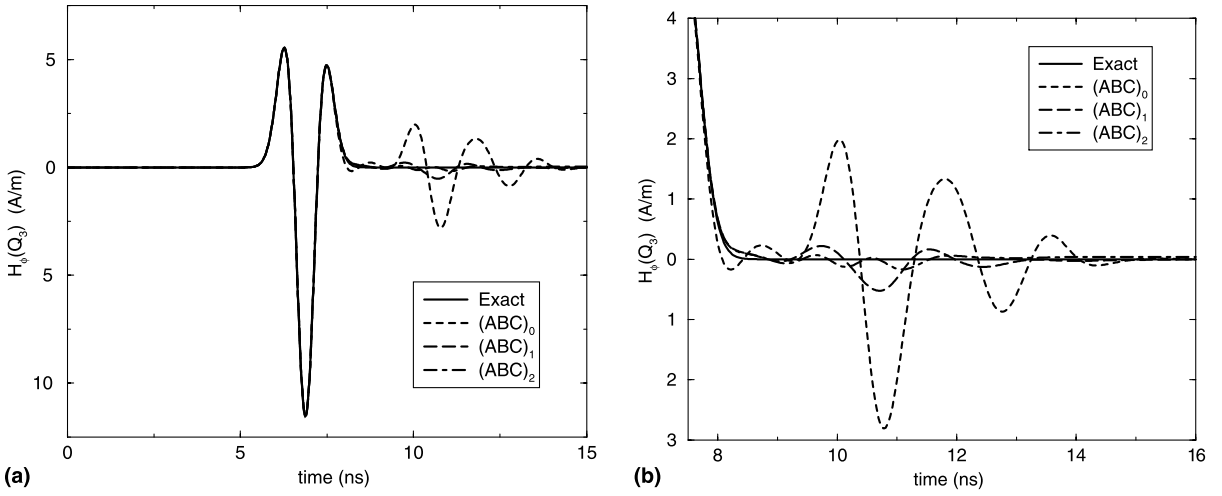

Fig. 5. Azimuthal magnetic field intensity at the point $(r, \theta) = (0.767, 166.8°)$ for the first three absorbing boundary conditions. Conventions are the same as in Fig. 3.

their plane wave reflection coefficients. For $(\mathrm{ABC})_2$ this improvement has been obtained at the cost of adding two new tangential vector unknowns ($\mathbf{p}$ and $\mathbf{P}_1$) at each quadrature point on the outer boundary for each of the 1350 cells in the outermost layer. In terms of resource requirements, it is roughly equivalent to adding field unknowns for another layer of cells beyond this boundary.

While these first tests do not allow generalizations about the behavior of error norms, they do indicate that the strategy of composing a convex outer boundary from flat facets is successful. High-order representations of the field unknowns in each cell can be matched with high-order absorbing boundary conditions of the Engquist–Majda type to reduce reflection errors. However, one should note that, after the exciting pulse has passed out of the computational domain, there will in general be some residual value for

the auxiliary functions $\mathbf{P}_k$ at each integration point on the outer boundary. These may give rise to long-term polynomial growth of $\mathbf{p}$ on the boundary, and therefore to inward-propagating waves at late times. Some evidence for this behavior has been found in our simulations, and a thorough investigation of the phenomenon is planned.

Acknowledgements

The authors acknowledge many helpful conversations with Professors David Gottlieb and Jan Hesthaven of Brown University and Professor Tim Warburton of the University of New Mexico. Professor Gottlieb's independent derivation of the second-order boundary condition (recently extended to arbitrary order with Ditkowski [16]) provided confirmation that these conditions might lead to practical numerical procedures. Thanks also are due to Professor Bertil Gustafsson of the University of Uppsala, who clarified several of the issues regarding weak instability for us in discussions with Professor Gottlieb at Brown. This work has been partially supported by the US Air Force under Contracts F33615-01-C-1866 and F49620-01-C-0015. The former contract includes funding from the Defense Advanced Research Projects Agency under the VET initiative, thanks to the efforts of Dr. Dennis Healy and Dr. Douglas Cochran. It is managed by Mr Jeffery Hughes of the Air Force Research Laboratory. The latter contract is with the Air Force Office of Scientific Research, and is managed by Dr. Arje Nachman. This work would not have reached its present stage without the continuing support and encouragement of both Mr. Hughes and Dr. Nachman.

References

[1] B. Engquist, A. Majda, Absorbing boundary conditions for the numerical simulation of waves, Math Comp. 31 (1977) 629.
[2] B. Engquist, A. Majda, Radiation boundary conditions for acoustic and elastic wave calculations, Commun. Pure Appl. Math. 32 (1979) 313.
[3] B. Cockburn, C.-W. Shu, The Runge–Kutta discontinuous Galerkin method for conservation laws V, J. Comput. Phys. 141 (1998) 199.
[4] J.S. Hesthaven, T. Warburton, Nodal high-order methods on unstructured grids. I. Time-domain solution of Maxwell's equations, J. Comput. Phys. 181 (2002) 186.
[5] G. Mur, Absorbing boundary conditions for the finite-difference approximation of the time domain electromagnetic field equations, IEEE Trans. Electromag. Compat. 23 (1981) 377.
[6] K.S. Yee, Numerical solution of initial boundary value problems involving Maxwell's equations in isotropic media, IEEE Trans. Antennas Propag. 14 (1966) 302.
[7] A. Taflove (Ed.), Advances in Computational Electromagnetics, Artech House, Norwood, MA, 1998, For a brief overview of the extensive literature on absorbing boundary conditions, see Section 1.3 and the references therein.
[8] J.-P. Berenger, A perfectly-matched layer for the absorption of electromagnetic waves, J. Comput. Phys. 114 (1994) 185.
[9] S. Abarbanel, D. Gottlieb, A mathematical analysis of the PML method, J. Comput. Phys. 134 (1997) 357.
[10] T. Hagstrom, Radiation boundary conditions for the numerical simulation of waves, Acta Numerica 8 (1999) 47.
[11] V. Shankar, A. Mohammadian, W. Hall, A time-domain finite-volume treatment for the Maxwell equations, Electromagnetics 10 (1990) 147.
[12] R. Higdon, Absorbing boundary conditions for difference approximations to the multidimensional wave equation, Math. Comput. 47 (1986) 437.
[13] R. Higdon, Numerical absorbing boundary conditions for the wave equation, Math. Comput. 49 (1987) 65.
[14] L. Halpern, L. Trefethen, Wide-angle one-way wave equations, J. Acoust. Soc. Am. 84 (1988) 1397.
[15] G-q. Zhang, High-order approximation of one-way wave equations, J. Comput. Math. 3 (1985) 90.
[16] A. Ditkowski, D. Gottlieb, On the Engquist–Majda absorbing boundary conditions for hyperbolic systems, in: Recent Advances in Scientific Computing and Partial Differential Equations, vol. 330, Contemporary Mathematics Series of the AMS, 2003.
[17] H.-O. Kreiss, Initial boundary value problems for hyperbolic systems, Commun. Pure Appl. Math. 23 (1970) 277.
[18] B. Gustafsson, Inhomogeneous conditions at open boundaries for wave propagation problems, Appl. Numer. Math. 4 (1988) 3.

[19] L. Trefethen, Instability of difference models for hyperbolic initial boundary value problems, Commun. Pure Appl. Math 37 (1994) 329.
[20] M.J. Grote, J.B. Keller, Nonreflecting boundary conditions for Maxwell's equations, J. Comput. Phys. 139 (1998) 327.
[21] D. Givoli, B. Neta, High-order non-reflecting boundary scheme for time-dependent waves, J. Comput. Phys. 186 (2003) 24.
[22] D.S. Jones, The Theory of Electromagnetism, Pergamon/Macmillan, New York, 1964, p.152.
[23] A.V. Kabakian, V. Shankar, W.F. Hall, Unstructured grid-based discontinuous Galerkin method for broadband electromagnetic simulations, J. Sci. Comput., to appear in 2004.